



OPEN ACCESS

ORIGINAL RESEARCH

Discovery of the gut microbial signature driving the efficacy of prebiotic intervention in obese patients

Julie Rodriguez ,¹ Sophie Hiel,¹ Audrey M Neyrinck ,¹ Tiphaine Le Roy ,^{1,2} Sarah A Pötgens,¹ Quentin Leyrolle,¹ Barbara D Pachikian,¹ Marco A Gianfrancesco,³ Patrice D Cani ,^{1,2} Nicolas Paquot,³ Miriam Cnop ,^{4,5} Nicolas Lanthier ,⁶ Jean-Paul Thissen,⁷ Laure B Bindels ,¹ Nathalie M Delzenne ¹

► Additional material is published online only. To view please visit the journal online (<http://dx.doi.org/10.1136/gutjnl-2019-319726>).

For numbered affiliations see end of article.

Correspondence to

Professor Nathalie M Delzenne, Metabolism and Nutrition Research Group, Louvain Drug Research Institute, Université Catholique de Louvain, Brussels, Belgium; nathalie.delzenne@uclouvain.be

Received 27 August 2019

Revised 15 January 2020

Accepted 17 January 2020

ABSTRACT

Objective The gut microbiota has been proposed as an interesting therapeutic target for metabolic disorders. Inulin as a prebiotic has been shown to lessen obesity and related diseases. The aim of the current study was to investigate whether preintervention gut microbiota characteristics determine the physiological response to inulin.

Design The stools from four obese donors differing by microbial diversity and composition were sampled before the dietary intervention and inoculated to antibiotic-pretreated mice (*hum-ob* mice; humanised obese mice). *Hum-ob* mice were fed with a high-fat diet and treated with inulin. Metabolic and microbiota changes on inulin treatment in *hum-ob* mice were compared with those obtained in a cohort of obese individuals supplemented with inulin for 3 months.

Results We show that *hum-ob* mice colonised with the faecal microbiota from different obese individuals differentially respond to inulin supplementation on a high-fat diet. Among several bacterial genera, *Barnesiella*, *Bilophila*, *Butyricimonas*, *Victivallis*, *Clostridium XIVa*, *Akkermansia*, *Raoultella* and *Blautia* correlated with the observed metabolic outcomes (decrease in adiposity and hepatic steatosis) in *hum-ob* mice. In addition, in obese individuals, the preintervention levels of *Anaerostipes*, *Akkermansia* and *Butyricoccus* drive the decrease of body mass index in response to inulin.

Conclusion These findings support that characterising the gut microbiota prior to nutritional intervention with prebiotics is important to increase the positive outcome in the context of obesity and metabolic disorders.

INTRODUCTION

The interaction between nutrients and the gut microbes is involved in the regulation of host metabolism, namely in the context of obesity and related metabolic diseases.¹ One interesting strategy to envisage weight control is the elaboration of nutritional interventions/recommendations with dietary fibres considered as prebiotics, defined as ‘substrates that are selectively utilized by host microorganisms conferring a health benefit’.^{2–7} The administration of inulin as prebiotic reduces adiposity and obesity-associated metabolic disorders in preclinical and human studies. Gut microbiota

Significance of this study

What is already known on this subject?

- Disturbances of the gut microbial ecosystem are associated with obesity and related metabolic disorders.
- The efficacy of dieting in obese patients is dependent on the initial gut microbiota composition.
- Supplementation with fermentable inulin-type dietary fibres leads to the improvement of obesity and related metabolic disorders, but the contribution of specific bacteria in the health improvement by inulin remains unknown.

What are the new findings?

- A dietary intervention with inulin in a multicentric cohort of obese patients reveals responders and non-responders in terms of improvement of body mass index and metabolic disorders.
- Improvement in metabolic disorders by inulin depends on the presence of specific consortia of bacteria but not on bacterial diversity.
- The transplantation of the gut microbiota from obese individuals to high-fat diet-fed mice reveals which changes of the gut microbiota are associated with the improvement of metabolic alterations by inulin and reveals key molecular targets involved in inulin effects on insulin sensitivity, steatosis and adiposity.

How might it impact on clinical practice in the foreseeable future?

- The efficacy of nutritional advice in the management of obesity is not optimal. We propose that the measurement of specific consortia of faecal bacteria can preclude the efficacy of prebiotic dietary fibres intervention in obese patients. Moreover, we have elucidated gut microbial bacteria that can be considered as new targets in the improvement of major metabolic alterations linked to obesity.

modulation by inulin-type fructans differ between individuals following the pattern of dietary fibre intake.⁸ However, in view of the existing data, it is difficult to evaluate which changes in the gut



© Author(s) (or their employer(s)) 2020. Re-use permitted under CC BY-NC. No commercial re-use. See rights and permissions. Published by BMJ.

To cite: Rodriguez J, Hiel S, Neyrinck AM, et al. Gut Epub ahead of print: [please include Day Month Year]. doi:10.1136/gutjnl-2019-319726

microbiota driven by inulin are involved in the improvement of obesity and metabolism in humans.^{9–14}

Gut microbiota characteristics explain the variable response toward several dietary interventions. Indeed, the initial gut microbiota influences the glycaemic response to real-life meals or bread as well as microbiota changes on resistant starch supplementation.^{15–17} A recent study highlighted that similar foods induced different effects on microbiome, suggesting that the interactions between diet and microbiome are personalised.¹⁸

In this context, we tested the hypothesis that the preintervention gut microbiota composition could influence the metabolic and microbial response to inulin supplementation in obese subjects. Faecal material was taken from obese individuals prior to intervention and transferred into microbiota-depleted mice (*hum-ob* for humanised obese mice). The metabolic and microbial response of *hum-ob* high-fat diet (HFD)-fed mice toward inulin supplementation was evaluated and compared with the response to inulin intervention in obese patients. We also analysed the preintervention characteristics of the gut microbiota that drive the improvement of body weight in obese patients treated with inulin (ClinicalTrials.gov identifier: NCT03852069).

METHODS

Additional protocols and complete procedures are described in the online supplementary material and methods section.

Experimental model and subject details

Mice

Specific pathogen-free (SPF) C57BL/6J male mice (Janvier Labs, Le Genest St Isle, France) were housed in a controlled environment (three per cage, 12 hours daylight cycle) with free access to food and water. Young mice (aged 4 weeks) were used to optimise the gut microbiota engraftment.¹⁹ Mice were divided into nine groups: one control group (SPF) and eight groups of mice inoculated with the faecal material of obese patients (*hum-ob*, figure 1A). According to previous procedures,^{19–20} the intestinal microbiota was first depleted by antibiotic treatment and cleansing with polyethylene glycol (PEG). Stool samples from four obese patients were inoculated three times (one time per day every 2 days). Control mice received water by gavage at the same time. After the first inoculation with stool samples, all groups of mice including the control mice were fed a HFD (45% kcal fat; E15744-347, ssniff, Soest, Germany) for 4 weeks. For each donor, one subgroup was supplemented with 0.2 g/day per mouse of native inulin (Fibruline, Cosucra, Pecq, Belgium) in the drinking water for 4 weeks.

Metabolic measurements

Plasma insulin and glucose were measured. The subcutaneous adipose tissue (SAT) was stained with H&E for adipocyte size quantification. Liver lipids were stained with oil red O; lipids were extracted from muscle gastrocnemius and liver prior enzymatic quantification. Protein extraction and immunoblotting of protein of interest were performed in liver and gastrocnemius muscle. Total RNA was isolated from different sections of SAT, brown adipose tissue (BAT), liver and skeletal muscle prior reverse transcriptase quantitative PCR (qPCR) analysis.²¹ The full procedures are detailed in online supplementary information.

Human cohort

The clinical intervention consisted of a 3-month, multicentric, single-blind, placebo-controlled randomised intervention in male and female obese patients (see online supplementary

section for inclusion and exclusion criteria). One hundred and six patients were randomised to receive either 16 g/day of native inulin (Cosucra, Belgium) or 16 g/day of maltodextrin (Cargill, Belgium). Fifty-five patients were randomised in the placebo group and 51 patients were assigned to the inulin group. Written informed consent was obtained from all participants before inclusion in the study.

Statistical analysis

Mice experiments: One-way analysis of variance (ANOVA) was performed between the SPF group and humanised untreated mice to evaluate the effect of faecal microbiota transfer (FMT), followed by a Tukey post hoc test. Effect of inulin supplementation was assessed using a Student's t-test between the two groups of mice colonised with the same donor.

Microbiota analysis: Significantly affected taxa or amplicon sequence variants (ASVs) by inulin were identified using a Welch's t-test in R, between untreated and treated groups for each donor. The p-value of the Welch's t-test was adjusted (q-value, significant if $q < 0.05$) to control for the false discovery rate (FDR) for multiple tests according to the Benjamini and Hochberg procedure.²²

Correlation between the variation of genera or ASVs significantly regulated by inulin and other metabolic variables was assessed by Spearman's correlation tests with an FDR correction. A significance level of $q < 0.05$ (adjusted p-value) was adopted for all analyses.

Human cohort: Responders and non-responders to inulin treatment were discriminated according to the body mass index (BMI) median value. Principal component analysis (PCA) and partial least square discriminant analysis (PLS-DA) models were built based on selected variables in R. For PLS-DA, a loading > 0.35 was chosen.

RESULTS

Characterisation of mice microbiota after FMT

We first selected four donors from the cohort of obese patients prior inulin intervention, who differed by the gut microbiota composition to perform FMT in antibiotic-PEG pretreated mice (figure 1A). Antibiotic-PEG efficiency was confirmed by the drastic decrease in total bacteria, supporting the elimination of more than 99.8% of faecal bacteria (figure 1B,C). Except for the SPF control group, all mice were recolonised by FMT with stools of obese patients. Donors were obese, drug-naïve diabetic or non-diabetic, displaying different faecal bacterial gene richness (Chao1 index, figure 1D) and differences in gut microbiota composition at the family level (figure 1E). The metabolic features also differed between donors, despite a similar BMI, as shown in online supplementary table 1. Four weeks after the FMT, similarities between the caecal microbiota of recipient mice and faecal microbiota composition of their respective donors were assessed. Unweighted UniFrac distance confirmed a different distribution between SPF and *hum-ob* mice (figure 1F), *hum-ob* mice gut microbiota being very close to their respective donors. Moreover, the level of *Faecalibacterium prausnitzii*, bacteria that are present in high proportion in humans but minimally in mice, clearly increased in all *hum-ob* mice, confirming that human bacteria colonised the recipient mice (figure 1G).

Differential response to inulin on body weight and adiposity in *hum-ob* mice

Despite similar food, water and inulin intake between groups (online supplementary figure 1A–C), the response to HFD in

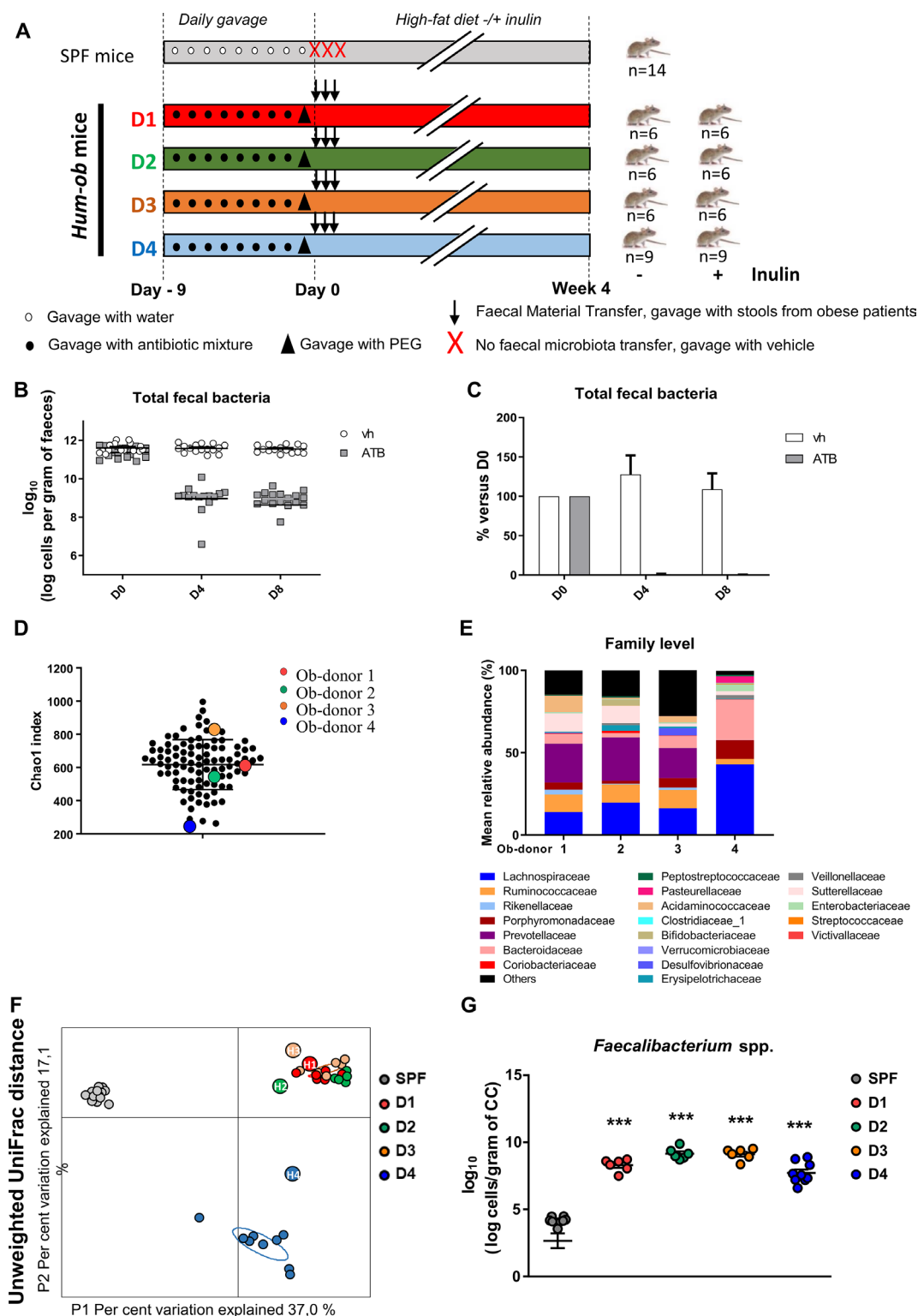


Figure 1 FMT from obese donors into antibiotic-pretreated mice. (A) Experimental design. (B and C) Total faecal bacteria analysed by qPCR in DNA extracted from faeces of antibiotic-treated mice at different time points (D0: before treatment, D4, D8: 4 or 8 days of antibiotic treatment). (B) Represents number of cells per gram of faeces. (C) Represents percentage of total faecal bacteria compared with D0. Results are expressed as mean \pm SEM. (D) α -diversity is estimated using the chao-1 index in the entire cohort, at baseline. Donors selected for FMT are represented by circles coloured red, green, orange and blue corresponding to donors 1, 2, 3 and 4, respectively. (E) Barplots for relative abundance of family levels accounting for more than 1% for each donor. (F) Principal coordinate analysis of the β -diversity index Unweighted UniFrac, coloured by mouse group. Small circles represent individual mice and larger circles represent human donors (D1, D2, D3, D4 for mice samples and H1, H2, H3, H4 for their respective human donor samples). (G) Quantification of *Faecalibacterium* spp by qPCR in DNA extracted from CC, 4 weeks after FMT. For five SPF mice, the levels remained undetectable. ***p<0.001 versus SPF mice (one-way ANOVA followed by Tukey post hoc test). ANOVA, analysis of variance; ATB, antibiotic treatment; CC, caecal content; FMT, faecal microbiota transfer; *hum-ob* mice, humanised obese mice; PEG, polyethylene glycol; qPCR, quantitative PCR; SPF, specific pathogen free; Vh, vehicle.

terms of body weight gain and adiposity differed between donors. Body weight significantly increased only in mice inoculated with stools from donor 1 (D1) compared with SPF mice and was restored by inulin supplementation only in this group (figure 2A). Regarding adiposity, FMT increased both SAT and epididymal adipose tissue in D1 *hum-ob* mice (figure 2B,C), whereas inulin supplementation reduced adiposity in D1 and D4 recipients. Visceral adipose tissue weight remained similar in all groups (figure 2D). In SAT, the mean adipocyte area was increased in D1 mice, an effect completely prevented by inulin (figure 2E,F). Gene expression was measured in adipose tissues (online supplementary table 2). Inulin treatment significantly reduced *cd11c* expression in both D1 and D4 *hum-ob* mice, suggesting that inulin reduced activated macrophage infiltration in SAT (figure 2G). Inulin also reduced the expression of inflammatory markers (*tnfa* and *ccl2*) in SAT of D1 recipients compared with untreated counterparts (figure 2G). In D1 *hum-ob* mice, inulin decreased mRNA levels of *cd36*, a fatty acid (FA) receptor. *Pparg* mRNA, regulating adipocyte differentiation and lipogenesis, decreased with inulin in both D1 and D4 *hum-ob* mice. In BAT, inulin specifically enhanced the expression of thermogenesis markers (*ucp1*, *prdm16* and *ppargc1a*) in D1 mice, a phenomenon that can promote FA oxidation (figure 2H; online supplementary table 2).

Inulin decreases hepatic lipid accumulation in D1 and D4 *hum-ob* mice

Inulin reduced lipid (triglyceride and cholesterol) accumulation only in D1 and D4 *hum-ob* (figure 3A–D). D1 mice had increased acetyl CoA carboxylase (ACC) phosphorylation on serine 79 residue, an effect further promoted by inulin and signing AMP-activated protein kinase (AMPK) activation²³ (figure 3E). Inulin also decreased nuclear sterol-regulatory element-binding proteins 1c and 2 (Srebp-1c and Srebp-2) in D1 and D4 mice (figure 3F,G). In D1 mice, inulin reduced *cd36* and *ppargc1a* mRNA, two proteins involved in FA uptake and oxidation (figure 3H), and mRNA levels of markers controlling triglycerides synthesis, such as *acaca*, *scd1*, *dgat2* and *elovl3* (figure 3H; online supplementary table 2). Inulin also decreased *scd1* and *dgat2* mRNA in D4 mice. These data suggest that inulin reduces hepatic lipid content in D1 and D4 mice by regulating the expression of genes involved in lipogenesis and FA oxidation.

Inulin improves muscle insulin sensitivity in D1 *hum-ob* mice

Biochemical analysis of gastrocnemius skeletal muscle highlighted an increase of intramuscular lipid and triglyceride content only in D1 *hum-ob* mice compared with SPF control mice, which was abrogated by inulin (figure 4A,B). In line with these findings, inulin robustly increased the phosphorylation of both protein kinase B, Akt (serine 473) and mammalian target of rapamycin, mTOR (serine 2448) in D1 *hum-ob* mice, indicating insulin signalling stimulation (figure 4C,D). As in the liver, inulin decreased *cd36* mRNA expression in the soleus of D1 mice. *Pparg* mRNA was increased in D1 muscle and decreased by inulin in both D1 and D4 *hum-ob* mice (figure 4E; online supplementary table 2). *Cpt1b* mRNA increase in *hum-ob* mice was counteracted by inulin in D1 mice only (figure 4E). Those data support that inulin improves insulin sensitivity in the muscle of D1 mice by decreasing FA uptake, limiting the availability of ligands of PPAR γ (peroxisome proliferator-activated receptor gamma). Notwithstanding these effects, we did not observe significant changes in fasting glycaemia and insulinaemia with the treatment (online supplementary figure 1D,E).

Inulin does not alter overall microbiota composition but induces donor-specific changes in microbiota composition

Caecal content and tissue weights were increased by inulin in all groups, signing a similar inulin fermentation (figure 5A,B). FMT decreased microbial α -diversity (Chao1 and Shannon indices) in all *hum-ob* mice, compared with control mice (figure 5C,D). Evenness dropped further with inulin in D2 and D4 mice. Unweighted UniFrac distance showed clusters due to interpersonal variation between donors (figure 5F).

Univariate analyses revealed that inulin induced donor-specific changes at the phylum and family level in *hum-ob* mice (figure 5E; online supplementary table S3). We also identified a subset of 18 genera differently regulated by inulin (FDR correction, q value <0.05), depending on the donor. Inulin increased *Bifidobacterium* and decreased *Barnesiella*, *Butyricimonas*, *Bilophila*, *Hungatella* and *Victivallis* in D1 mice (online supplemental table S4). In D2 mice, *Alistipes*, *Coprobacter* and *Parabacteroides* decreased with inulin, whereas *Bacteroides* increased. In D3 mice, inulin decreased *Paraprevotella* and *Murimonas*. In D4, inulin increased *Parabacteroides*, *Clostridium XIVa*, *Raoultella*, *Blautia* and *Akkermansia* and decreased *Bacteroides*, *Clostridium XVIII* and *Oscillibacter*. In addition, the analysis of ASVs showed that the most abundant ASV and related genera are similarly regulated by inulin (online supplemental table S4). In addition, three ASVs belonging to *Ruminococcus 2*, *Parasutterella* and *Collinsella*, respectively, were decreased by inulin in D2 mice and one ASV from *Desulfovibrio* genus decreased with inulin in D3 group (online supplemental table S5). Forty other ASVs not be classified at the genus level were modified by inulin, including one ASV from Enterobacteriaceae family that largely decreased on inulin in all *hum-ob* mice (ASV12; online supplemental table S5). Highly abundant ASV5 from Firmicutes and the unclassified ASV7 also dramatically decreased on inulin treatment in some *hum-ob* mice.

Some specific bacteria, known to be regulated by inulin, were also quantified by qPCR. FMT clearly decreased the level of *Lactobacillus* spp and increased *Faecalibacterium* spp in all *hum-ob* mice (online supplementary figure 2D,E). Inulin increased total bacteria and *Bifidobacterium* spp in D1 and D4 groups (online supplementary figure 2A,B). *Roseburia* spp was increased by inulin in all *hum-ob* mice (online supplementary figure 2C). Finally, inulin specifically raised the levels of *Faecalibacterium* spp, *Lactobacillus* spp and *Akkermansia muciniphila* in D4 mice (online supplementary figure 2D–F).

Correlation analysis between the most significant metabolic effects and the 18 genera regulated by inulin was performed. Among several correlations identified (q -value <0.05), some genera positively correlated with hepatic lipid accumulation (*Barnesiella*, *Butyricimonas*, *Bilophila*, *Hungatella* and *Victivallis*) and are those significantly decreased by inulin in D1 mice, the group exhibiting the better metabolic response to inulin (figure 5; online supplementary table S4). Moreover, the four genera negatively correlated with hepatic lipid content (*Clostridium XIVa*, *Raoultella*, *Blautia* and *Akkermansia*) were specifically increased in D4 mice, the second inulin-responder group of mice. Correlation analysis was also performed between biological parameters and all ASVs modulated by inulin and belonging to other genera or unclassified as genus. ASV218 from *Desulfovibrio* negatively correlated with *cd36* level in SAT (online supplementary figure 3). The other unclassified ASVs correlated with metabolic features were not similarly regulated by inulin in D1 and D4 groups. Only the ASV12 was regulated in all *hum-ob* mice but did not correlate with biological parameters (online supplementary table S5 and online supplementary figure 3).

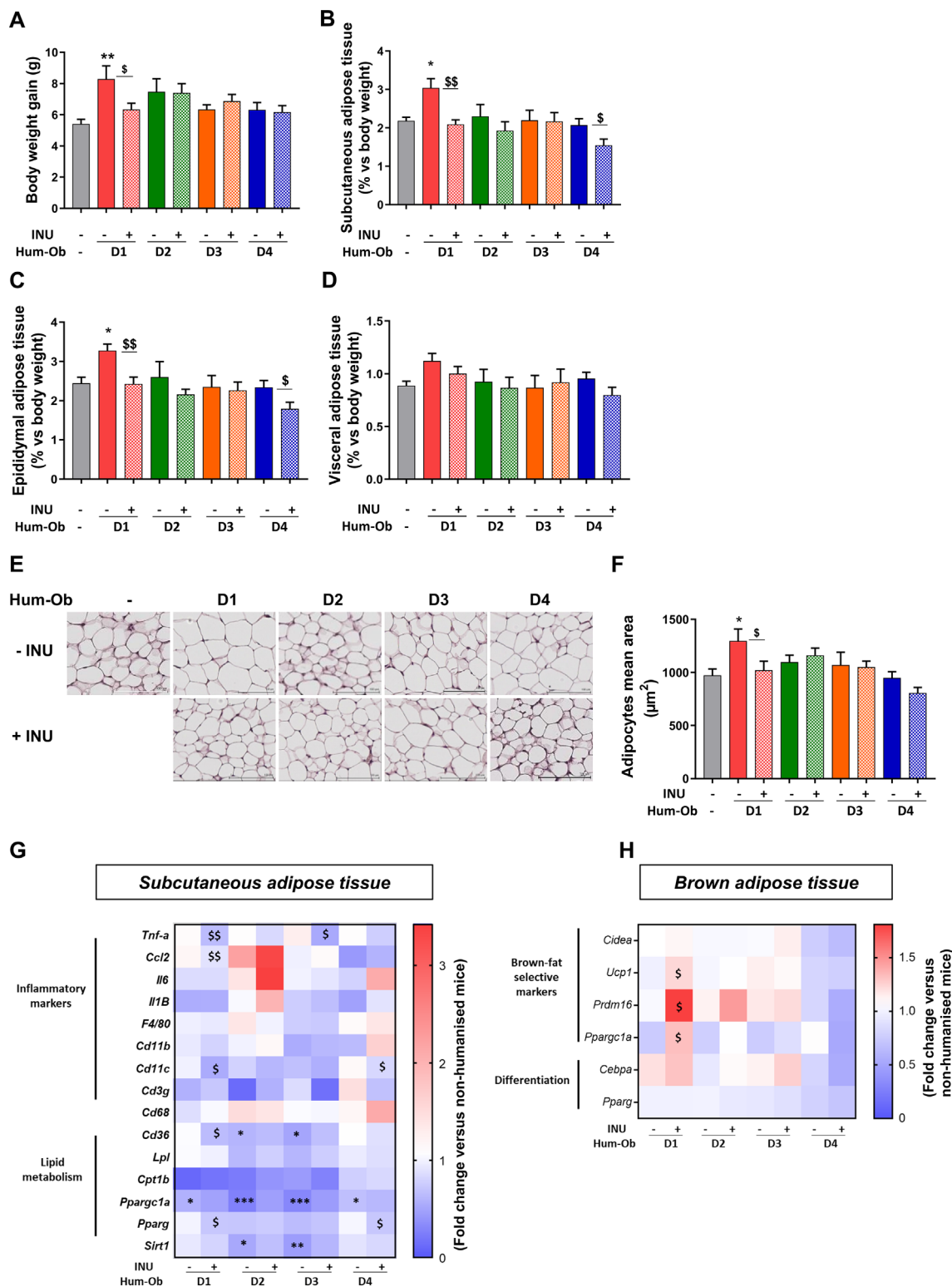


Figure 2 Differential response on body weight gain and adiposity with inulin in *hum-ob* mice. Mice were fed a HFD for 4 weeks following the FMT and supplemented or not with inulin. (A) Body weight gain for SPF and humanised mice supplemented or not with inulin. (B–D) Weight of subcutaneous, epididymal and visceral adipose tissues. (E) Representative H&E-stained pictures of SAT. Scale bar=100 μm . (F) Adipocyte mean area (μm^2) in SAT. (G and H) Gene expression measured by qPCR in SAT and BAT. The data are presented as fold change of expression level versus the level measured in tissue of SPF mice (mean SPF group=1, see also online supplementary table 2). For each analysis, results are expressed as mean \pm SEM. FMT effect: * p <0.05, ** p <0.01 and *** p <0.001 for untreated *hum-ob* mice versus SPF mice (one-way ANOVA followed by a Tukey post hoc test). Inulin effect: $^{\$}$ p <0.05 and SS p <0.01 for comparison between the group receiving inulin and their counterpart for each donor (Student's *t*-test). ANOVA, analysis of variance; BAT, brown adipose tissue; FMT, faecal microbiota transfer; HFD, high-fat diet; *hum-ob* mice, humanised obese mice; INU, inulin; qPCR, quantitative PCR; SAT, subcutaneous adipose tissue; SPF, specific pathogen free.

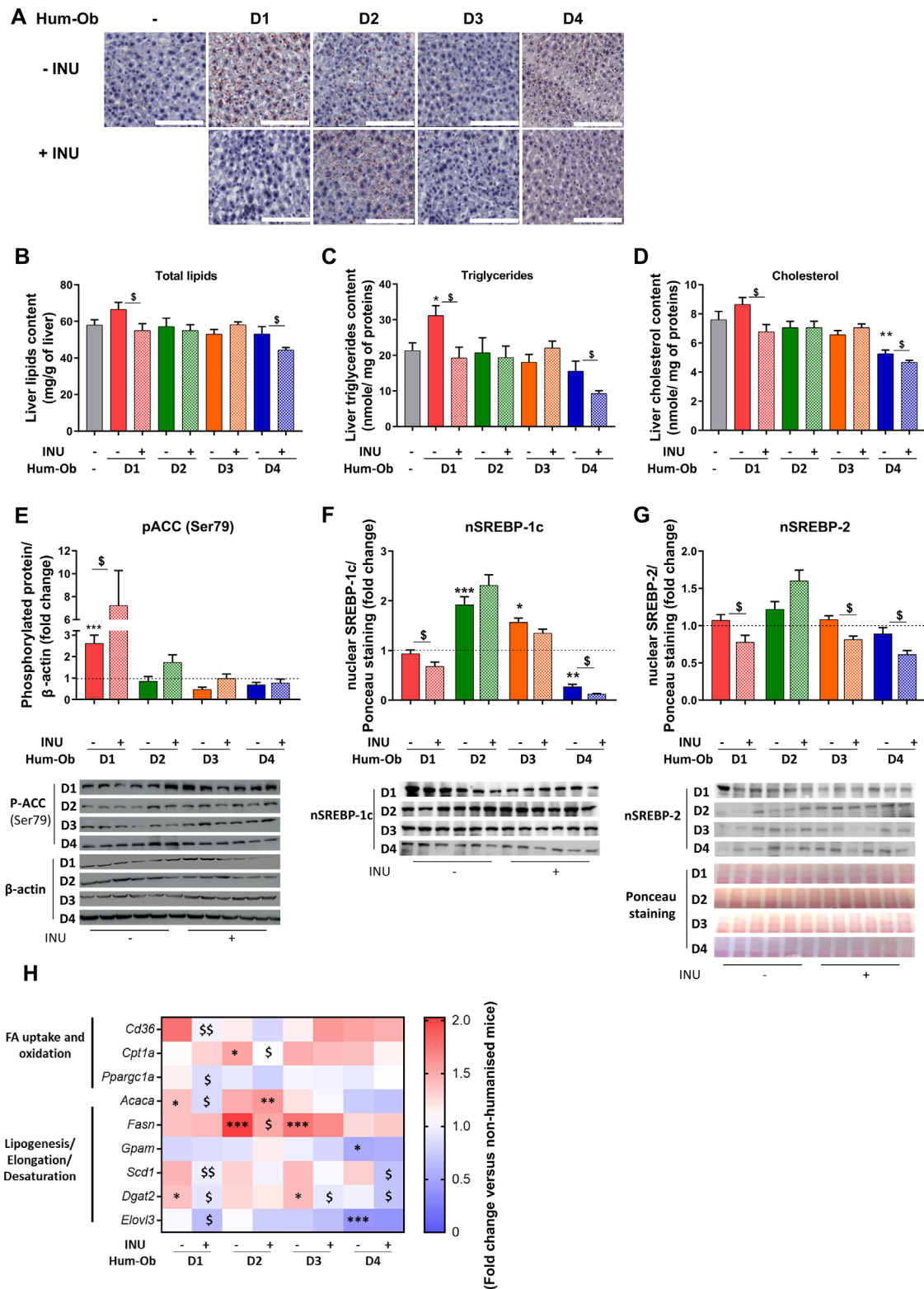


Figure 3 Inulin decreases hepatic lipid accumulation in D1 and D4 *hum-ob* mice. (A) Histochemical detection of neutral lipids in liver sections, scale bar=100 μ m. (B–D) Total lipid, triglyceride and cholesterol contents of the liver. Data are expressed as mean \pm SEM. (E–G) Immunoblotting and quantification of pACC, and nuclear expression of Srebp-1c or Srebp2. β -actin or Ponceau staining was used as protein loading control. The black dotted line represents the mean obtained for SPF mice. Data are expressed as mean \pm SEM. (H) Gene expression measured by qPCR in liver. The data are presented as fold change of expression levels in tissue of SPF mice (mean SPF group=1, see also online supplementary table 2). For each analysis, results are expressed as mean \pm SEM. FMT effect: * p <0.05, ** p <0.01 and *** p <0.001 for untreated *hum-ob* mice versus SPF mice (one-way ANOVA followed by a Tukey post hoc test). Inulin effect: $^{\$}$ p <0.05 and 55 p <0.01 for comparison between the group receiving inulin and their counterpart for each donor (Student's *t*-test). ACC, acetyl coA carboxylase; ANOVA, analysis of variance; FA, fatty acid; FMT, faecal microbiota transfer; *hum-ob* mice, humanised obese mice; INU, inulin; pACC, phospho-acetyl coA carboxylase; qPCR, quantitative PCR; SPF, specific pathogen free; Srebp: sterol-regulatory element-binding protein.

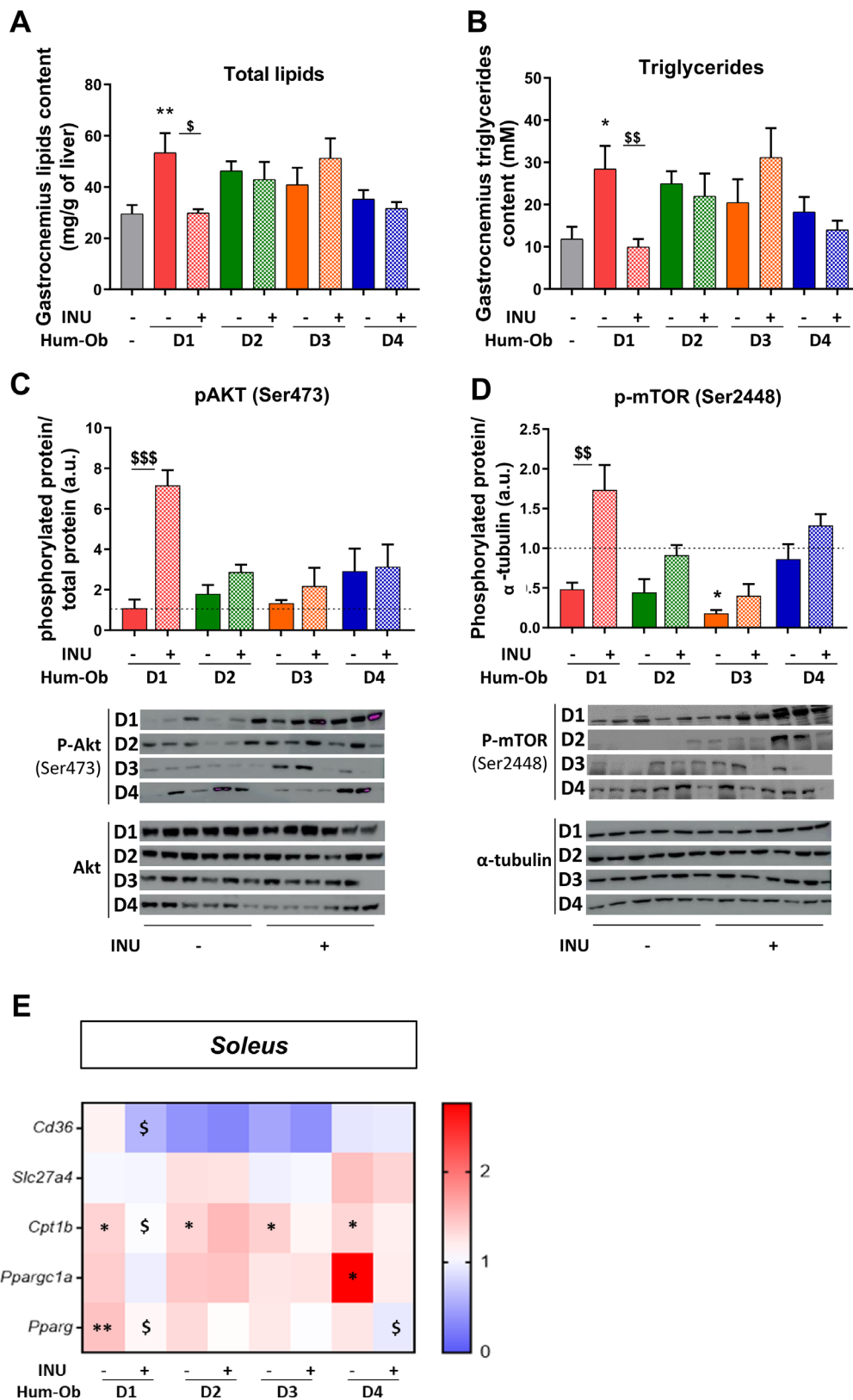


Figure 4 Inulin improves muscle insulin sensitivity in D1 *hum-ob* mice. (A and B) Total lipid and triglyceride content in the gastrocnemius muscle. (C and D) Immunoblotting and quantification of the ratio of pAkt to total Akt protein and p-mTOR to α -tubulin. The black dotted line represents the mean obtained for SPF mice. Data are expressed as mean \pm SEM. (E) Gene expression measured by qPCR in soleus muscle. The data are presented as fold change of expression levels in tissue of SPF mice (mean SPF group=1, see also online supplementary table 2). For each analysis, results are expressed as mean \pm SEM. FMT effect: * p <0.05 and ** p <0.01 for untreated *hum-ob* mice versus SPF mice (one-way ANOVA followed by a Tukey post hoc test). Inulin effect: $^{\$}$ p <0.05, $^{\$\$}$ p <0.01 and $^{$$$}$ p <0.001 for comparison between the group receiving inulin and their counterpart for each donor (Student's t-test). ANOVA, analysis of variance; FMT, faecal microbiota transfer; *hum-ob* mice, humanised obese mice; INU, inulin; pAkt, phospho-protein kinase B; p-mTOR, phospho-mammalian target of rapamycin qPCR, quantitative PCR; SPF, specific pathogen free.

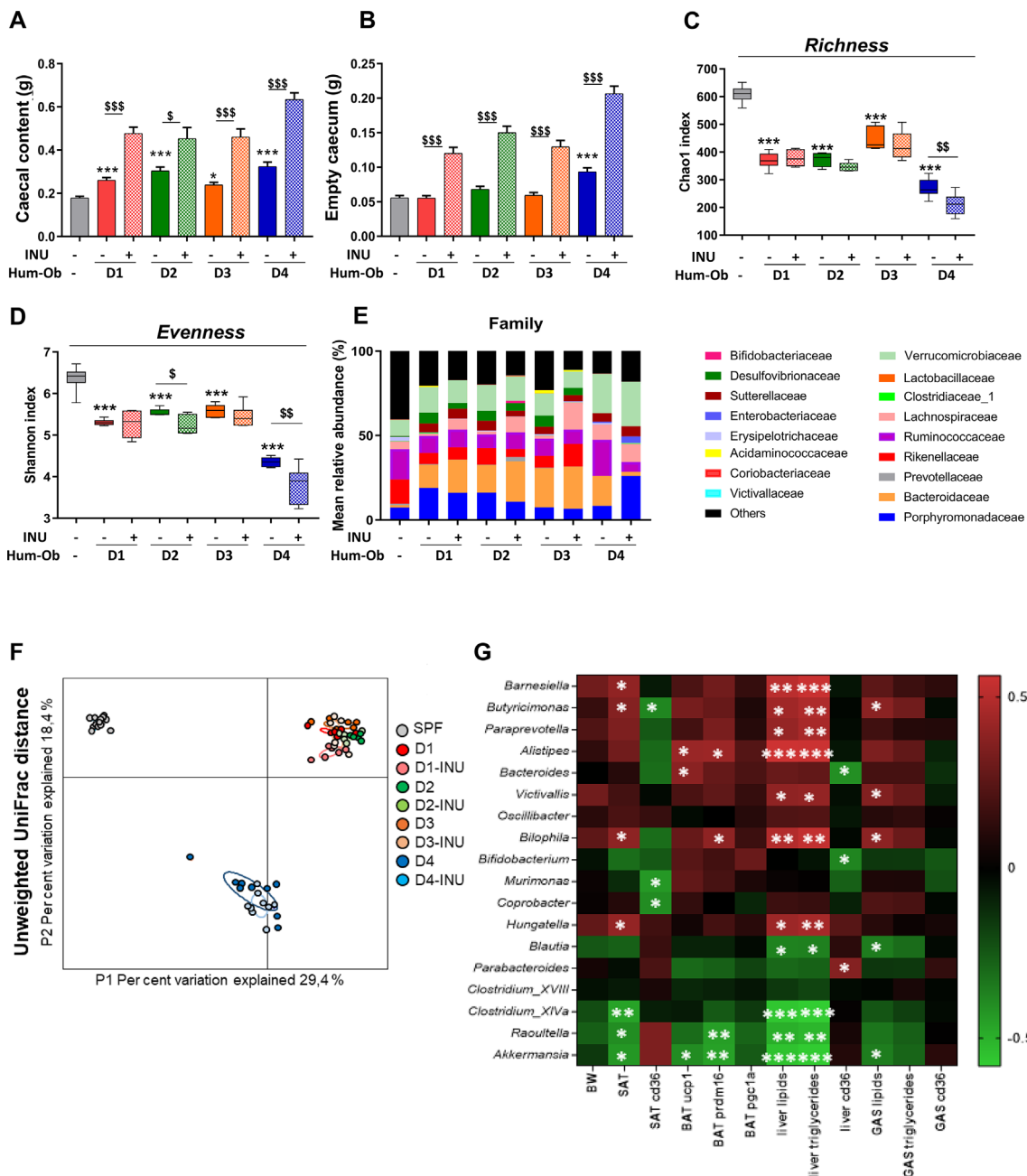


Figure 5 Inulin does not alter overall microbiota composition but induces donor-specific changes. (A and B) Caecal content and tissue weight. (C and D) Measure of alpha-diversity indexes: chao-1 and Shannon. (A–D) Data are expressed as mean±SEM. The effect of FMT was calculated using a one-way ANOVA followed by a Tukey post hoc test, * $p < 0.05$ and *** $p < 0.001$ for untreated *hum-ob* mice versus SPF mice. The effect of inulin was then calculated using a Student’s t-test, $^{\$}p < 0.05$ and $^{SS}p < 0.001$ for comparison between the group receiving inulin and their counterpart for each donor. (E) Barplots of relative abundance of family levels accounting for more than 1%, for each group. (F) Principal coordinate analysis of the β -diversity index Unweighted UniFrac, coloured by mice group. (G) Heatmap of Spearman’s correlations between genera significantly modified by inulin treatment (FDR correction, q value) and the most significant metabolic changes observed with inulin. * $q < 0.05$, ** $q < 0.01$ and *** $q < 0.001$ for significant correlations between parameters. ANOVA, analysis of variance; BAT, brown adipose tissue; BW, body weight; FDR, false discovery rate; FMT, faecal microbiota transfer; GAS, gastrocnemius muscle; *hum-ob* mice, humanised obese mice; INU, inulin; SAT, subcutaneous adipose tissue; SPF, specific pathogen free.

Microbiota-related criteria drive the metabolic response to inulin treatment in *hum-ob* mice and in humans

The model of FMT in mice did not allow to identify the bacteria that could be implicated in body weight changes. For this, we used the whole human cohort of obese patients treated with inulin, to verify whether some bacteria could be linked to the BMI regulation by inulin.

Donors used for FMT have been enrolled in a large clinical intervention on the impact of 3-month inulin supplementation (16g/day) in obese patients, combined with dietary advice to consume vegetables enriched in inulin-type fructans. The impact of inulin treatment in donors was consistent with the response in *hum-ob* mice: donor 1 had better clinical measures after inulin, including decreased BMI and fat mass, improved hepatic steatosis

Table 1 General characteristics and metabolic variables of obese donors during intervention

Donor	D1		D2		D3		D4	
	Baseline	13 weeks						
BMI (kg/m ²)	40.45	35.5	41.56	40.9	42.24	40.25	42.16	44.14
Weight (kg)	112.8	99	113.6	110	117.6	113.6	108.6	113.7
Waist/hip ratio	0.93	0.88	0.92	0.85	0.89	0.88	0.89	0.96
Systolic BP (mm Hg)	140	120	145	142	142	160	120	130
Diastolic BP (mm Hg)	80	80	100	90	100	110	80	80
Lean mass (%)	50	57	55	57	54	51	55	54
Fat mass (%)	50	43	45	43	46	49	45	46
Fasting glycaemia (mg/dL)	108	94	99	100	96	100	102	99
Fibroscan elasticity (kPa)	6.2	4.9	3.6	3.8	3.4	3.6	3.9	5.4
Fibroscan CAP (dB/m)	307	234	325	355	275	309	359	375
HbA1c (%)	6.1	5.8	6.2	6.2	5.6	5.5	5.8	5.9
AST (U/l)	19	17	25	21	15	12	22	23
ALT (U/l)	22	29	36	25	20	17	29	37
gGT (U/l)	14	11	38	30	37	40	20	25
CRP (ng/mL)	5455	1384	6420	10432	10970	17830	3619	7718
Energy intake (kcal/day)	1725	1249	2083	1791	1810	1361	1875	2307
Fibres (g/day)	20.1	36.7	23.6	35.7	32.6	50.1	12.8	20.5
Fructans (g/day)	0.26	4.79	0.90	10.16	4.82	24.85	0.15	2.31
Proteins (g/day)	54.3	56.7	90.2	78.6	78	52.8	77.4	65.2
Lipids (g/day)	62.2	60.3	86.6	55.4	70.9	49.1	82.5	105.6
Carbohydrates (g/day)	226	106.4	228	229.4	156.6	138.7	199.1	259.8
IPAQ continuous score (physical activity)	132	973	2040	2580	945	1670	3004	1350

ALT, alanine aminotransferase; AST, aspartate aminotransferase; BMI, body mass index; BP, blood pressure; CRP, C reactive protein; gGT, gamma glutamyl-transferase; HbA1c, glycated haemoglobin; IPAQ, International Physical Activity Questionnaire.

and decreased energy intake (table 1). For donors 2 and 3, despite a loss of 3–4 kg, no metabolic or anthropometric changes were observed. Surprisingly, for donor 4, the effect of inulin differed from the *hum-ob* mice since inulin did not improve fat mass or hepatic lipid accumulation (table 1). Actually, donor 4 largely increased her energy intake as lipids and carbohydrates, and reduced her physical activity during the intervention. This probably explains the different impact of inulin between mice and donor.

At the end of the intervention, we subdivided participants in the inulin arm (n=51), according to the median of the BMI change into non-responders (unchanged BMI) and responders (decreased BMI; figure 6A). Chao1 index, reflecting the richness of the gut microbiota, was similar between non-responder and responder groups (figure 6B). Surprisingly, PCA using the variation (difference between baseline and 3-month intervention) of all bacterial genera during the clinical intervention did not allow to separate non-responders and responders (figure 6C). Interestingly, the PCA taking into account only the variation of genera with inulin highlighted in *hum-ob* mice (ie, 18 genera identified by taxonomic analysis + 4 with ASV analysis) tended to separate non-responder and responder groups (Monte Carlo test, p=0.06, figure 6D). The PLS-DA, based on the variation of the same subset of genera (identified in mice) during the human protocol, indicated that the main variations responsible for the different BMI response seem to be the increase in *Bifidobacterium* spp associated with a decrease in *Collinsella*, *Barnesiella*, *Akkermansia* and *Bilophila* in responders (figure 6E). Univariate analysis confirmed a significant decrease in *Collinsella* and *Akkermansia* in responders compared with non-responders (figure 6F). To assess whether some genera could predict the response to inulin, we performed a PLS-DA analysis based on all genera present before the intervention (figure 6G). A

clear separation was observed between non-responders and responders; among the main variables (loading >0.35) responsible for this specific clustering, we found some genera outlined above, such as *Collinsella*, *Bifidobacterium*, *Akkermansia*, *Bacteroides* and other new genera such as *Butyrivicoccus* that seems highly present in responders (figure 6G). Univariate analysis only show a significant higher basal presence of *Akkermansia* and *Butyrivicoccus* and a lower level of *Anaerostipes* in responders, compared with non-responders. These data support that a subset of bacteria involved in the specific response to inulin probably plays an important role in the interindividual response in terms of BMI observed in the human cohort.

DISCUSSION

Inulin-type fructans have been proposed as an interesting dietary fibre with prebiotics properties, since many animal data and some intervention studies with inulin support their potential interest in the management of body weight and obesity-related diseases. The link with the gut microbiota changes occurring on inulin intervention remains elusive.²⁴ A previous study demonstrated that short-chain fructans decreased the body weight gain, fat mass accumulation and increased caecal content in axenic mice inoculated with stools from one healthy lean adult.²⁵ The authors propose that the results may depend on the human gut microbiota used for the inoculation and may not be generalisable. We show in our study that the inulin response is highly variable across ‘humanised’ mice colonised with the stools from different obese patients, providing evidence that the gut microbiota composition prior to intervention influences the health outcome. For this, we inoculated mice with samples from different obese donors, and body weight gain of *hum-ob* mice on HFD was differently affected by inulin, even when mice

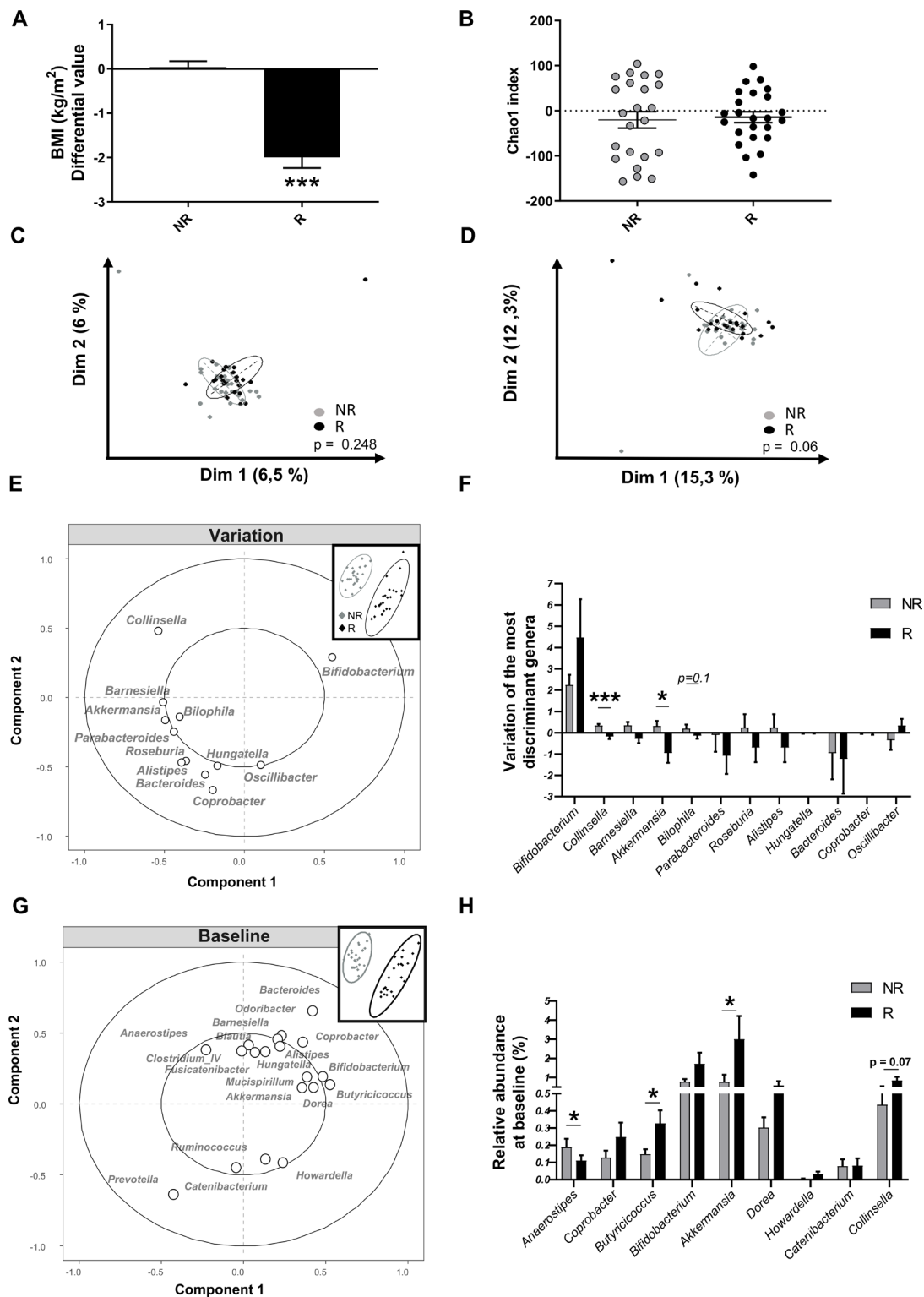


Figure 6 Intervention study with inulin in a multicentric human cohort reveals inulin responders (R) and non-responders (NR) in term of body mass index (BMI) improvement and changes in the gut microbiota. (A) Variation of BMI, after 3 months of intervention, in the inulin arm: NR (n=26) and R (n=25) patients were separated using the median change in BMI. ***p<0.001 versus placebo and ^{SSS}p<0.001 versus NR. (B) Chao1 index (alpha-diversity) in NR (n=23) and R (n=24). (C–D) Principal component analysis of the gut microbiota composition based on all the genera (C) or selected genera (D) in NR and R patients. Statistical analysis was assessed by a Monte Carlo rank test. (E) Partial least square discriminant analysis (PLS-DA) of the variation of selected genera (selection from the humanised obese mice (*hum-ob*) mice model) during the intervention with inulin in NR and R patients. (F) Variation of the most discriminant genera after 3 months of intervention. Data are expressed as mean±SEM and analysed with a Mann-Whitney test in R compared with NR subjects. (G) PLS-DA of all genera, before the intervention, in NR and R patients. The main variables (cut-off: 0.1% of relative abundance, loadings >0.35) explaining the clustering are represented. (H) Relative abundance of bacterial genera, at baseline, selected (by the previous PLS-DA and the *in vivo* model of *hum-ob* mice) in NR and R patients. Data are expressed as mean±SEM and analysed with a Mann-Whitney test in R compared with NR subjects.

exhibit the same dietary behaviour. Inulin differently regulated metabolic changes in adipose tissues, liver and skeletal muscle. Finally, the observed interindividual variability was accompanied by specific gut microbiota changes with inulin in *hum-ob* mice.

In two groups of mice (D2 and D3), inulin had no effect, whereas the two other groups (D1 and D4) responded with a positive impact of inulin, the metabolic improvement being more prominent in D1. The two groups of responders in mice received the gut microbiota from one diabetic donor (D1) and one pre-diabetic donor (D4), but mice receiving stools from another diabetic donor (D2) did not respond to inulin supplementation, suggesting that the diabetic status is not the main driver of the metabolic response to inulin. However, this hypothesis must be challenged in future intervention studies with a large number of patients with diabetes versus without diabetes. In D1 mice, FMT exacerbated the impact of HFD, and inulin counteracted the majority of these effects such as body weight and fat gain and hepatic and muscular lipid accumulation. Recent study demonstrated that the response of gut microbiota to resistant starch-containing dietary supplement differed depending on the initial gut microbiota from healthy donors used to inoculate mice.²⁶ In our study, we could recapitulate the importance of the selective changes in microbiota to explain the metabolic response to inulin (online supplementary figure 4). In D1 group, inulin preferentially decreased bacteria positively correlated with detrimental metabolic features. Among them, inulin decreased *Bilophila* and *Barnesiella* and increased *Bifidobacterium* genera. In conventional mice fed a HFD, prebiotic treatment led to an increase in *Bifidobacterium* spp associated with a decrease in *Bilophila*.²⁷ Vandeputte *et al* also demonstrated that inulin selectively increases *Bifidobacterium* and decreased *Bilophila* in mildly constipated individuals, an effect linked to improved constipation-related quality of life.²⁸ Our data support that, in humanised mice, the changes of those bacteria is important to get interesting health effects, even beyond the context of obesity. Interestingly, the strong effect of inulin in D1 mice was also observed for the donor 1 during the intervention. Even if it is clear that the increase of physical activity by donor 1 could improve metabolic parameters during the intervention, the *hum-ob* mice model supports that the gut microbiota from this donor is favourable for metabolic response to inulin.

In D4 mice, even if FMT did not aggravate the impact of HFD, inulin improved fat mass and hepatic steatosis. In this group, inulin preferentially upregulated bacteria known to be associated with beneficial effects on host metabolism,^{29 30} such as *A. muciniphila*, which negatively correlated with fatty liver in our study. In agreement, it has been shown that *Akkermansia* administration prevents the development of obesity and reverses metabolic disorders in HFD-fed mice.^{29 30} Interestingly, the responder group from the whole cohort was characterised by a higher abundance of *Akkermansia* at baseline, but its abundance decreased on intervention. Dao *et al* also showed that obese subjects with a higher abundance of *Akkermansia* at baseline had a greater improvement in metabolic alterations during a low-caloric diet intervention, but *Akkermansia* was also decreased in this group during the intervention.³¹ This suggests that the higher abundance of *Akkermansia* prior to intervention could determine the successful rate of dietary intervention, but that an increase in *Akkermansia* on inulin treatment is not the driver for the metabolic improvement.

In D4 mice, inulin also increased the levels of *Faecalibacterium* spp, *Lactobacillus* spp and *Bifidobacterium* spp. This was consistent with previous works showing that *F. prausnitzii* is lower in obese patients and in patients with diabetes and increases after

weight loss.^{32 33} Moreover, inulin-type fructans intervention versus placebo increased *Bifidobacterium* spp and *Faecalibacterium* in a cohort of obese women.¹⁴ Finally, improvement of obesity and metabolic disorders was also observed during probiotic intervention studies with *Lactobacillus* species.^{34 35}

The biological effects of inulin in D1 and D4 *hum-ob* mice shared some similarities but not all. Inulin reduced hepatic lipid content by decreasing nuclear expression of *srebp1* and *srebp2* proteins and mRNA expression of lipogenic genes in both groups. Previous data showed that genes involved in lipogenesis, FA elongation and desaturation were decreased in mice colonised with a simplified human gut microbiota, and treated with inulin.³⁶ In D1 mice, we found that these changes could be mediated by a regulation in hepatic ACC phosphorylation by inulin, controlling both FA synthesis and oxidation.²³ However, in D4 mice, the mechanism appeared to be ACC-independent. This suggests that an inulin intervention may drive improvement of steatosis and hepatic diseases, but depending on the initial microbiome, the molecular mechanism behind it could be different. Decreased muscle triglyceride content and improved insulin sensitivity was only observed in D1 *hum-ob* mice, confirming a different response pattern between the two responder groups. Once again, linking the gut microbial changes to inulin response shows a positive correlation between *Butyrivibrio*, *Victivallis* and *Bilophila* with myosteatosis, three genera decreased by inulin in D1 mice.

Among several hypotheses explaining the variable response to nutrients, and more specifically to inulin, different basal gut microbial diversity or basal *Bifidobacterium* level have been proposed as criteria. In our study, the richness *chao1* index was similar at baseline and inulin did not modify it neither in *hum-ob* mice, nor in the human cohort. Previous studies suggested an inverse correlation between the initial faecal bifidobacterial numbers and the magnitude of increase of bifidobacteria with inulin or oligofructose-enriched inulin in healthy humans,^{8 37 38} suggesting that inulin might induce a greater metabolic response in individuals with lower bifidobacteria at baseline. In our human cohort, the baseline level of *Bifidobacterium* spp was not lower in responders. Actually, only three genera were significantly different at baseline between responders and non-responders (*Anaerostipes*, *Akkermansia* and *Butyrivibrio*), even if other bacteria at baseline seem to drive the separation between both groups (PLS-DA analysis). We believe that the magnitude of response could be influenced by a subset of bacteria (rather than one specific bacterium) simultaneously affected by prebiotics. Consistent with this, Zhao *et al* demonstrated that a set of short-chain fatty acid (SCFA)-producing bacteria was promoted by dietary fibres and was key to improve host glycaemic control.³⁹ They identified 15 strains of SCFA producers, belonging to *Faecalibacterium*, *Lactobacillus*, *Bifidobacterium* or *Ruminococcus* genera, which were suggested to exert beneficial effects on the one hand and keep detrimental bacteria away on the other. Accordingly, we found increased *F. prausnitzii*, *Lactobacillus* spp and *Bifidobacterium* genus in one group of responder mice.

The current data highlight that specificities of the gut microbiota drive the metabolic and microbial response to inulin. Choosing a specific nutritional strategy to manage non-alcoholic fatty liver disease, glucose homeostasis or adiposity would require to pay more attention not only on the initial gut microbiota but also on the potency of the gut microbiota to be modified adequately by specific prebiotics. In our study, the patient D4 met all the 'microbial criteria' to respond to inulin intervention but it was unsuccessful for this patient, because

he did not follow dietary and behavioural advices. The consequence was an increase in body weight and fat mass, which could counteract the potential beneficial effect of inulin on metabolic disorders.

This means that a successful dietary intervention, namely with prebiotics, has to be considered as one of the tools to improve metabolic health but patient's motivation remains crucial. One limitation of our study could be that all human donors were women, whereas the transplantation of the faecal material was performed in male mice only. This was motivated by the fact that all previous experiments testing inulin in HFD mice had been performed in male mice that are more prone to develop metabolic disorders than the female ones.^{40–41} In addition, no difference was observed in terms of improvement of BMI on inulin treatment following the gender in the human cohort (data not shown).

In conclusion, a personalised approach should be developed for prebiotic interventions to target obese patients prone to have a favourable response and to avoid discouraging negative outcomes. The identification of bacterial consortia within this complex ecosystem that drive the metabolic response towards prebiotics is of particular interest to implement adequate nutritional advices for personalised management of metabolic disorders in obesity.

Author affiliations

¹Metabolism and Nutrition Research Group, Louvain Drug Research Institute, Université catholique de Louvain, Brussels, Belgium

²WELBIO- Wallon Excellence in Life Sciences and BIOTEchnology, UCLouvain, Université catholique de Louvain, Brussels, Belgium

³Laboratory of Diabetology, Nutrition and Metabolic disease, Université de Liège, Liège, Belgium

⁴ULB Center for Diabetes Research, Université Libre de Bruxelles, Brussels, Belgium

⁵Division of Endocrinology, Erasmus Hospital, Université Libre de Bruxelles, Brussels, Belgium

⁶Service d'Hépatogastroentérologie, Cliniques Universitaires Saint-Luc, Brussels, Belgium

⁷Département de Diabetologie et Nutrition, Institut de recherche expérimentale et clinique, Université catholique de Louvain, Brussels, Belgium

Twitter Julie Rodriguez @JulieRdz1213, Tiphaine Le Roy @Titicaccae, Patrice D Cani @MicrObesity and Laure B Bindels @Laure_Bindels

Acknowledgements We thank Remi Selleslagh, Véronique Allaëys, Isabelle Blave and Bouazza Es Saadi for their precious implication in the study. We thank the UCLouvain's platform "Support en méthodologie et calcul statistique" and more specifically Céline Bugli and Lieven Desmet for their helpful advice concerning statistical analyses. We also thank Coralie Frenay, Marie Barea and Marjorie Fadeur, the dieticians involved in the clinical trial.

Contributors JR and NMD conceived and designed the experiments, interpreted the data and wrote the manuscript. JR performed the experiments and data analysis. AMN and LBB participated to design and to experiments. TLR designed the FMT protocol. JR, SH, BDP, MAG, MC, NP, NL and J-PT participated to the acquisition of the clinical data. AMN, TLR, SAP, QL and LBB participated to the analysis and interpretation of data. AMN, PDC, MC, NP, NL, J-PT and LBB provided intellectual input on the paper and reviewed the paper. NMD supervised the overall project.

Funding This research is supported by the competitive cluster Wagralim from Wallonia (FOOD4GUT 518 project, convention 1318148). NMD is a recipient of grants from Wallonia (FOOD4GUT project; 519 FiberTAG project from European Joint Programming Initiative 'A Healthy Diet for a Healthy 520 Life') and from Belgium National Scientific Research Fund (FRS-FNRS; convention PDR 521 T.0068.19). PDC is a senior research associate at FRS-FNRS (Fonds de la Recherche 522 Scientifique), Belgium, and supported by the Funds Baillet Latour (Grant for Medical Research 523 2015). TLR is a postdoc fellow funded by FRFS-WELBIO (WELBIO-CR-2017C-02).

Competing interests None declared.

Patient consent for publication Not required.

Ethics approval Trial registered at ClinicalTrials.gov as NCT03852069 was approved by the Comité d'éthique Hospitalo-facultaire de Saint-Luc'.

Provenance and peer review Not commissioned; externally peer reviewed.

Data availability statement For the gut microbiota analysis, raw sequences can be accessed in Sequence Read Archive database (SRA accession numbers PRJNA594535, PRJNA595949).

Open access This is an open access article distributed in accordance with the Creative Commons Attribution Non Commercial (CC BY-NC 4.0) license, which permits others to distribute, remix, adapt, build upon this work non-commercially, and license their derivative works on different terms, provided the original work is properly cited, appropriate credit is given, any changes made indicated, and the use is non-commercial. See: <http://creativecommons.org/licenses/by-nc/4.0/>.

ORCID iDs

Julie Rodriguez <http://orcid.org/0000-0002-8271-3893>

Audrey M Neyrinck <http://orcid.org/0000-0002-9435-3338>

Tiphaine Le Roy <http://orcid.org/0000-0002-0874-1490>

Patrice D Cani <http://orcid.org/0000-0003-2040-2448>

Miriam Cnop <http://orcid.org/0000-0002-5112-1692>

Nicolas Lanthier <http://orcid.org/0000-0002-7651-9314>

Laure B Bindels <http://orcid.org/0000-0003-3747-3234>

Nathalie M Delzenne <http://orcid.org/0000-0003-2115-6082>

REFERENCES

- Sonnenburg JL, Bäckhed F. Diet-microbiota interactions as moderators of human metabolism. *Nature* 2016;535:56–64.
- Gentile CL, Weir TL. The gut microbiota at the intersection of diet and human health. *Science* 2018;362:776–80.
- Romani-Pérez M, Agustí A, Sanz Y. Innovation in microbiome-based strategies for promoting metabolic health. *Curr Opin Clin Nutr Metab Care* 2017;20:1–91.
- Delzenne NM, Cani PD, Everard A, et al. Gut microorganisms as promising targets for the management of type 2 diabetes. *Diabetologia* 2015;58:2206–17.
- Druart C, Alligier M, Salazar N, et al. Modulation of the gut microbiota by nutrients with prebiotic and probiotic properties. *Adv Nutr* 2014;5:624S–33.
- Delzenne NM, Olivares M, Neyrinck AM, et al. Nutritional interest of dietary fiber and prebiotics in obesity: lessons from the MyNewGut Consortium. *Clin Nutr* 2019. doi:10.1016/j.clnu.2019.03.002. [Epub ahead of print: 09 Mar 2019].
- Gibson GR, Hutkins R, Sanders ME, et al. Expert consensus document: the International scientific association for probiotics and prebiotics (ISAPP) consensus statement on the definition and scope of prebiotics. *Nat Rev Gastroenterol Hepatol* 2017;14:491–502.
- Healey G, Murphy R, Butts C, et al. Habitual dietary fibre intake influences gut microbiota response to an inulin-type fructan prebiotic: a randomised, double-blind, placebo-controlled, cross-over, human intervention study. *Br J Nutr* 2018;119:176–89.
- Zou J, Chassaing B, Singh V, et al. Fiber-Mediated Nourishment of gut microbiota protects against diet-induced obesity by restoring IL-22-mediated colonic health. *Cell Host Microbe* 2018;23:41–53.
- Dewulf EM, Cani PD, Neyrinck AM, et al. Inulin-type fructans with prebiotic properties counteract GPR43 overexpression and PPAR γ -related adipogenesis in the white adipose tissue of high-fat diet-fed mice. *J Nutr Biochem* 2011;22:712–22.
- Salazar N, Dewulf EM, Neyrinck AM, et al. Inulin-type fructans modulate intestinal Bifidobacterium species populations and decrease fecal short-chain fatty acids in obese women. *Clin Nutr* 2015;34:501–7.
- Reimer RA, Willis HJ, Tunnicliffe JM, et al. Inulin-type fructans and whey protein both modulate appetite but only fructans alter gut microbiota in adults with overweight/obesity: a randomized controlled trial. *Mol Nutr Food Res* 2017;61. doi:10.1002/mnfr.201700484. [Epub ahead of print: 29 Oct 2017].
- Roberfroid M, Gibson GR, Hoyles L, et al. Prebiotic effects: metabolic and health benefits. *Br J Nutr* 2010;104 Suppl 2:S1–63.
- Dewulf EM, Cani PD, Claus SP, et al. Insight into the prebiotic concept: lessons from an exploratory, double blind intervention study with inulin-type fructans in obese women. *Gut* 2013;62:1112–21.
- Zeevi D, Korem T, Zmora N, et al. Personalized nutrition by prediction of glycemic responses. *Cell* 2015;163:1079–94.
- Korem T, Zeevi D, Zmora N, et al. Bread affects clinical parameters and induces gut Microbiome-Associated personal glycemic responses. *Cell Metab* 2017;25:1243–53.
- Venkataraman A, Sieber JR, Schmidt AW, et al. Variable responses of human microbiomes to dietary supplementation with resistant starch. *Microbiome* 2016;4:33.
- Johnson AJ, Vangay P, Al-Ghalith GA, et al. Daily sampling reveals personalized Diet-Microbiome associations in humans. *Cell Host Microbe* 2019;25:789–802.
- Le Roy T, Debédât J, Marquet F, et al. Comparative evaluation of microbiota engraftment following fecal microbiota transfer in mice models: age, kinetic and microbial status matter. *Front Microbiol* 2018;9:3289.
- Reikvam DH, Erofeev A, Sandvik A, et al. Depletion of murine intestinal microbiota: effects on gut mucosa and epithelial gene expression. *PLoS One* 2011;6:e17996.
- Olivares M, Rodriguez J, Pötgens SA, et al. The Janus face of cereals: Wheat-Derived prebiotics counteract the detrimental effect of gluten on metabolic homeostasis in mice fed a high-fat/high-sucrose diet. *Mol Nutr Food Res* 2019;63:e1900632:1900632.

- 22 Benjamini YHY. Controlling the False Discovery Rate : A Practical and Powerful Approach to Multiple Testing. *J Royal Statistic Soc* 1995;57:289–300.
- 23 Viollet B, Foretz M, Guigas B, *et al.* Activation of AMP-activated protein kinase in the liver: a new strategy for the management of metabolic hepatic disorders. *J Physiol* 2006;574:41–53.
- 24 Cerdó T, García-Santos JA, G Bermúdez M, *et al.* The role of probiotics and prebiotics in the prevention and treatment of obesity. *Nutrients* 2019;11. doi:10.3390/nu11030635. [Epub ahead of print: 15 Mar 2019].
- 25 Respondek F, Gerard P, Bossis M, *et al.* Short-Chain fructo-oligosaccharides modulate intestinal microbiota and metabolic parameters of humanized gnotobiotic diet induced obesity mice. *PLoS One* 2013;8:e71026.
- 26 Cherbuy C, Bellet D, Robert V, *et al.* Modulation of the caecal gut microbiota of mice by dietary supplement containing resistant starch: impact is donor-dependent. *Front Microbiol* 2019;10:1234.
- 27 Everard A, Lazarevic V, Gaia N, *et al.* Microbiome of prebiotic-treated mice reveals novel targets involved in host response during obesity. *Isme J* 2014;8:2116–30.
- 28 Vandeputte D, Falony G, Vieira-Silva S, *et al.* Prebiotic inulin-type fructans induce specific changes in the human gut microbiota. *Gut* 2017;66:1968–74.
- 29 Everard A, Belzer C, Geurts L, *et al.* Cross-Talk between Akkermansia muciniphila and intestinal epithelium controls diet-induced obesity. *Proc Natl Acad Sci U S A* 2013;110:9066–71.
- 30 Plovier H, Everard A, Druart C, *et al.* A purified membrane protein from Akkermansia muciniphila or the pasteurized bacterium improves metabolism in obese and diabetic mice. *Nat Med* 2017;23:107–13.
- 31 Dao MC, Everard A, Aron-Wisnewsky J, *et al.* Akkermansia muciniphila and improved metabolic health during a dietary intervention in obesity: relationship with gut microbiome richness and ecology. *Gut* 2016;65:426–36.
- 32 Remely M, Hippe B, Zanner J, *et al.* Gut microbiota of obese, type 2 diabetic individuals is enriched in Faecalibacterium prausnitzii, Akkermansia muciniphila and Peptostreptococcus anaerobius after weight loss. *Endocr Metab Immune Disord Drug Targets* 2016;16:99–106.
- 33 Furet J-P, Kong L-C, Tap J, *et al.* Differential adaptation of human gut microbiota to bariatric surgery-induced weight loss: links with metabolic and low-grade inflammation markers. *Diabetes* 2010;59:3049–57.
- 34 Park S-S, Lee Y-J, Song S, *et al.* Lactobacillus acidophilus NS1 attenuates diet-induced obesity and fatty liver. *J Endocrinol* 2018;237:87–100.
- 35 Le Barz M, Daniel N, Varin TV, *et al.* In vivo screening of multiple bacterial strains identifies Lactobacillus rhamnosus Lb102 and Bifidobacterium animalis ssp. lactis Bf141 as probiotics that improve metabolic disorders in a mouse model of obesity. *Faseb J* 2019;33:4921–35.
- 36 Weitekunat K, Schumann S, Petzke KJ, *et al.* Effects of dietary inulin on bacterial growth, short-chain fatty acid production and hepatic lipid metabolism in gnotobiotic mice. *J Nutr Biochem* 2015;26:929–37.
- 37 Kolida S, Meyer D, Gibson GR. A double-blind placebo-controlled study to establish the bifidogenic dose of inulin in healthy humans. *Eur J Clin Nutr* 2007;61:1189–95.
- 38 de Preter V, Vanhoutte T, Huys G, *et al.* Baseline microbiota activity and initial bifidobacteria counts influence responses to prebiotic dosing in healthy subjects. *Aliment Pharmacol Ther* 2008;27:504–13.
- 39 Zhao L, Zhang F, Ding X, *et al.* Gut bacteria selectively promoted by dietary fibers alleviate type 2 diabetes. *Science* 2018;359:1151–6.
- 40 Stubbins RE, Najjar K, Holcomb VB, *et al.* Oestrogen alters adipocyte biology and protects female mice from adipocyte inflammation and insulin resistance. *Diabetes Obes Metab* 2012;14:58–66.
- 41 Stubbins RE, Holcomb VB, Hong J, *et al.* Estrogen modulates abdominal adiposity and protects female mice from obesity and impaired glucose tolerance. *Eur J Nutr* 2012;51:861–70.

Supplementary material and methods section

METHODS

Animals

C57BL/6J male mice (4 weeks old, Janvier Labs, Le Genest St Isle, France) were housed in groups of 3 per cage in a controlled environment (12-h daylight cycle) with free access to food and water. The experiment was approved by and performed following the guidelines of the local ethics committee for animal care of the Health Sector of Université catholique de Louvain under the specific agreement number 2017/UCL/MD/005. Housing conditions were as specified by the Belgian Law of 29 May 2013 regarding the protection of laboratory animals (Agreement no LA 1230314). Every effort was made to minimize animal pain, suffering, and distress. As shown in the figure 1A, mice were divided into nine groups: one control SPF group and eight groups of mice that were humanized by inoculating gut microbiota from obese patients.

Antibiotic therapy: According to previous procedures^{1,2}, we depleted the intestinal microbiota in the eight groups of humanized mice, by using eight days of antibiotic treatment. The antibiotic mixture consisting of ampicillin (10 mg/mL), neomycin (10 mg/mL), metronidazol (8 mg/mL), vancomycin (5 mg/mL) was administered by daily gavage. The first three days of antibiotic gavage was also supplemented with amphotericin B (30 µL/mL). Antibiotic treatment was then followed a bowel cleansing with polyethylene glycol (PEG). SPF mice were daily gavage with water during the antibiotic treatment.

FMT: following the antibiotic treatment and PEG administration (except for the SPF), all groups of mice were inoculated three times with a gavage of stool samples from four obese patients (SPF group received the vehicle). The inoculum containing stool samples from donors was diluted in an anoxic ringer-cystein buffer. The four groups of mice inoculated with the stool samples from the four donors are identified as *hum-ob* mice (for humanized obese mice). SPF mice were force-fed with the same volume of vehicle buffer.

Experiment: after the first inoculation with stool samples, all groups of mice including the SPF mice were fed a high-fat diet (45% kcal fat, E15744-347, Ssniff, Soest, Germany) for four weeks. For each donor, one subgroup of *hum-ob* mice was supplemented or not with 0.2 g/day per mouse of native inulin (Fibruline®, Cosucra, Pecq, Belgium) in the drinking water for the four weeks. Food intake and water consumption were recorded twice a week.

Human cohort

The clinical intervention was a 3-month, multicentric, single-blind, placebo-controlled randomized intervention in male and female obese patients. The protocol was performed in three university hospitals in Belgium (Cliniques Universitaires of St-Luc from Brussels, ULB Erasme Hospital from Brussels and Centre Hospitalier Universitaire from Liège). The inclusion criteria were: BMI >30 kg/m², age 18-65 years, Caucasian ethnicity, presence of at least one metabolic disorder associated with obesity (prediabetes/diabetes, dyslipidemia, hypertension, non-alcoholic fatty liver disease). The exclusion criteria included use of antibiotics, pro/prebiotics, fibers as a dietary supplement, or any molecule that modifies intestinal transit time within 6 weeks before starting the study. 106 patients were randomized to consume either 16 g/day of native inulin (Cosucra, Belgium) or 16 g/day of maltodextrin (Cargill, Belgium). 55 patients were randomized in the placebo group and 51 patients were assigned to the inulin group. In addition, patients were asked to consume, at least once a day, a recipe based on vegetables enriched or not in inulin-type fructans. A dietician performed a one-week recall questionnaire to evaluate energy intake at baseline and at the end of the intervention. Physical activity was evaluated by IPAQ questionnaire. Anthropometric measures were assessed at baseline and after three months of intervention, i.e. weight, height, waist and hip circumference, blood pressure, body composition (using bioimpedance devices BIA 101, Akern, Italy; Biocorpus, Medi Cal, Germany; Tanita BC-418 MA, Tanita,

UK). Fibroscan assessed liver stiffness (fibrosis) and controlled attenuation parameter (steatosis). This study was approved by the "Comité d'éthique Hospitalo-facultaire de Saint-Luc". Written informed consent was obtained from all participants before inclusion in the study. This trial was registered at clinicaltrials.gov as NCT03852069.

Metabolic measurements

Lipid content was measured in the liver and gastrocnemius muscle tissues after extraction with chloroform-methanol according to the Folch method³. Blood glucose levels were determined, after 6 hours of fasting, using a glucose meter (Roche Diagnostics) on 3.5 µl of blood collected from the tail vein. Blood sample was also harvested at the same time to assess plasma insulin concentrations. Plasma insulin concentrations were determined using an ultrasensitive ELISA kit (Mercodia, Uppsala, Sweden).

RNA Extraction and real-time quantitative PCR

Total RNA was isolated from tissues using the TriPure isolation reagent kit (Roche Diagnostics, Penzberg, Germany). Complementary DNA was prepared by reverse transcription of 1 µg total RNA using the Kit Reverse Transcription System (Promega, Madison, WI). Real-time polymerase chain reaction (PCR) was performed with a CFX96 Touch Real-Time PCR Detection System and software (Biorad Laboratories Ltd, UK) using SYBR Green (Applied Biosystems, The Netherlands and Eurogentec, Verviers, Belgium) for detection. All samples were run in duplicate in a single 96-well reaction plate, and data were analyzed according to the $2^{-\Delta\Delta CT}$ method. The purity of the amplified product was verified by analyzing the melting curve performed at the end of amplification. The ribosomal protein L19 (RPL19) gene was chosen as a reference gene.

Histology

Measurement of mean adipocytes area: adipocytes area were measured after hematoxylin and eosin staining of the subcutaneous adipose tissue slices. Adipocytes area were quantified using the ImageJ software. At least 500 adipocytes were analyzed per mouse.

Hepatic lipid staining: frozen liver sections were sliced at 5 µm, stained with oil red O and scanned (Leica SCN400; Leica, Wetzlar, Germany). The lipid area was determined on whole sections using the imaging software TissueIA (version 2.0.3, Leica Biosystems, Dublin, Ireland). Pixels corresponding to the oil red O staining were selected to create a color profile. Total tissue area was defined by setting the tissue intensity threshold at 210 (grey value). Results were expressed as stained area (below threshold)/tissue area (below threshold). Two representative tissue pieces were analyzed for each mouse.

Protein extraction and immunoblotting

For total protein extraction: 50mg of liver or gastrocnemius muscle were placed in ice-cold buffer [20 mM Tris, 270 mM sucrose, 5 mM EGTA, 1 mM EDTA, 1% Triton X-100, 1 mM sodium orthovanadate, 50 mM sodium β-glycerophosphate, 5 mM sodium pyrophosphate, 50 mM sodium fluoride, 1 mM 1,4-dithiothreitol (DTT), and 10% protease inhibitor cocktail 10X (Roche Applied Science, Vilvoorde, Belgium)] and then homogenized using a TissueLyser device (Qiagen). Homogenates were centrifuged at 10,000 g for 10 min at 4 °C. Supernatants were collected and stored at -80°C.

For nuclear protein extraction: nuclear proteins were extracted following manufacturer's instruction (NE-PER, Thermo Scientific, Waltham, MA, USA) from 50 mg of liver.

50µg of total proteins were denatured by mixing with Laemmli buffer and linearization was achieved by heating the samples for 5 min at 100°C. The samples were loaded with prestained molecular mass markers (Thermo Fisher Scientific). The proteins were then separated on SDS-polyacrylamide gels and transferred to a PVDF membrane. Membranes were then blocked in Tris-buffered saline with 0.1% v/v Tween 20 (TBST) containing 5% of non-fat dried milk. Membrane were incubated overnight with the following primary antibodies (1:1000 dilution in TBST containing 1% of bovine serum albumin): phospho-

ACC (Ser79), phospho-Akt (Ser473), Akt, phospho-mTOR (Ser2448) from Cell Signaling, Srebp1c from Thermo Scientific, Srebp2 and β -actin from Abcam. Membranes were then incubated with a secondary antibody (1:1000 diluted in TBST containing 5% of non-fat dried milk) conjugated to horseradish peroxidase from Cell Signaling Technology. β -actin, α -tubulin or Ponceau staining were used as loading control and all results were expressed relative to the SPF conventional mice. Signals were revealed using ECL Western blotting substrates (SuperSignal West Pico Substrate, Thermo Scientific). Gels are analyzed and quantified by ImageQuant[®] TL instrument and software version 8.1 (GE Healthcare, Buckinghamshire, England).

DNA Extraction and 16S rRNA Gene Sequencing

Mice and donor subset:

DNA was extracted from the mouse cecal content and donor stool samples using a QIAamp DNA Stool Mini Kit (Qiagen, Hilden, Germany) including a bead-beating step.

Cohort subset:

Stool samples were available for 47 patients on 51 assigned to the inulin group, during the clinical intervention. Stool samples were collected at baseline and after 3 months of intervention and stored at room temperature with a DNA stabilizer (Stratec biomolecular, Berlin, Germany) for maximum three days, then transferred to -80°C for the analysis of the gut microbiota composition. Genomic DNA was extracted from feces using a PSP[®] spin stool DNA kit (Stratec biomolecular, Berlin, Germany).

Amplicon sequencing of the microbiome was done at the University of Minnesota Genomics Center. Briefly, the V5-V6 region of the 16S rRNA gene was PCR-enriched using the primer pair V5F_Nextera (TCGTCGGCAGCGTCAGATGTGTATAAGAGACAGRGGATTAGATACCC) and V6R_Nextera (GTCTCGTGGGCTCGGAGATGTGTATAAGAGACAGCGACRRCCATGCANACCT) in a 25 μ l PCR reaction containing 5 μ l of template DNA, 5 μ l of 2X HotStar PCR master mix, 500 nM of final concentration of primers and 0.025 U/ μ l of HostStar Taq+ polymerase (QIAGEN). PCR-enrichment reactions were conducted as follow, an initial denaturation step at 95°C for 5 min followed by 25 cycles of denaturation (20 s at 98°C), annealing (15 s at 55°C), and elongation (1 min at 72°C), and a final elongation step (5 min at 72°C). Next, the PCR-enriched samples were diluted 1:100 in water for input into library tailing PCR. The PCR reaction was analogous to the one conducted for enrichment except with a KAPA HiFi Hot Start Polymerase concentration of 0.25 U/ μ l, while the cycling conditions used were as follows, initial denaturation at 95°C for 5 min followed by 10 cycles of denaturation (20 s at 98°C), annealing (15 s at 55°C), and elongation (1 min at 72°C), and a final elongation step (5 min at 72°C). The primers used for tailing are the following: F-indexing primer AATGATACGGCGACCACCGAGATCTACAC[i5]TCGTCGGCAGCGTC and R-indexing primer CAAGCAGAAGACGGCATACGAGAT[i7]GTCTCTGTTGCTCGG, where [i5] and [i7] refer to the index sequence codes used by Illumina. The resulting 10 μ l indexing PCR reactions were normalized using a SequalPrep normalization plate according to the manufacturer's instructions (Life Technologies). 20 μ l of each normalized sample was pooled into a trough, and a SpeedVac was used to concentrate the sample pool down to 100 μ l. The pool was then cleaned using 1X AMPureXP beads and eluted in 25 μ l of nuclease-free water. The final pool was quantitated by QUBIT (Life Technologies) and checked on a Bioanalyzer High-Sensitivity DNA Chip (Agilent Technologies) to ensure correct amplicon size. The final pool was then normalized to 2 nM, denatured with NaOH, diluted to 8 pM in Illumina's HT1 buffer, spiked with 20% PhiX, and heat denatured at 96°C for 2 minutes immediately prior to loading. A MiSeq 600 cycle v3 kit was used to sequence the pool.

Subsequent bioinformatics and biostatistics analyses were performed *in house*. Initial quality filtering of the reads was performed with the Illumina Software, yielding an average of 168312 (for the mice and donor subset) and 111507 (for the human cohort subset) pass-filter reads per sample. Quality scores were visualized with the FastQC software (<http://www.bioinformatics.babraham.ac.uk/publications.html>), and reads were trimmed to 220 bp (R1) and 200 bp (R2) with the FASTX-Toolkit (http://hannonlab.cshl.edu/fastx_toolkit/). Next, reads were merged with the merge-illumina-pairs application v1.4.2 (with P = 0.03, enforced Q30 check, perfect matching to primers which are removed by the software, and otherwise default settings including no ambiguous nucleotides allowed)⁴. For mice

and donor analysis, for all the samples but two, a subset of 29000 reads was randomly selected using Mothur v1.25.0⁵, to avoid large disparities in the number of sequences. In the human cohort subset, a subset of 25000 reads was randomly selected. Subsequently, the UPARSE pipeline implemented in USEARCH⁶ was used to further process the sequences. Amplicon sequencing variants (ASVs) were identified using UNOISE3. The analysis allowed the identification of 1937 ASVs for the mouse and donor subset and 3305 ASVs for the cohort subset. Taxonomic prediction was performed using the *nbc_tax* function, an implementation of the RDP Naive Bayesian Classifier algorithm⁷. The phylotypes were computed as percent proportions based on the total number of sequences in each sample. Alpha diversity indexes and beta diversity indexes were calculated using QIIME⁸. PCoA plot of the beta-diversity indexes were visualized using R software.

For the mice subset, significantly affected taxa by inulin were identified using a Welch's t-test in R, for each donor. The p-value of the Welch's t-test was then adjusted (q-value) to control for the false discovery rate (FDR) for multiple tests according to the Benjamini and Hochberg procedure⁹.

Raw sequences can be accessed in SRA database (accession numbers PRJNA594535, PRJNA595949).

LEGENDS

Supplemental Figure 1. Dietary intake and metabolic parameters.

(A) Daily food intake in grams per mouse. (B) Daily water intake per mouse in milliliters. (C) Daily inulin intake per mouse in grams. (D) Fasted plasma glucose (mg.dl⁻¹). (E) Fasted plasma insulin (mg.L⁻¹).

Supplemental Figure 2. Gut microbiota composition analysed by qPCR in DNA extracted from caecal content.

(A) Total bacteria (B) *Bifidobacterium* spp. (C) *Roseburia* spp. (D) *Faecalibacterium* spp. (E) *Lactobacillus* spp. (F) *Akkermansia muciniphila*. A circle is used for each mouse, a square represents the level of bacteria found in the feces of the human obese donor. For each analysis, results are expressed as mean \pm SEM., *p<0,05 and ***p<0,001 for untreated *hum-ob* mice versus SPF mice., §p<0,05, §§p<0,01 and §§§p<0,001 for comparison between the group receiving inulin and their counterpart for each donor.

Supplemental Figure 3. Several ASVs are correlated with metabolic features in *hum-ob* mice.

Heatmap of Spearman's correlations between ASVs significantly modified by inulin treatment (FDR correction, q value) and the most significant metabolic changes observed with inulin. *q<0,05, **q<0,01 and ***q<0,001 for significant correlations between parameters. Analysis was performed using ASVs present at 0.1% of relative abundance in at least one sample.

Supplemental Figure 4. Schematic representation of the microbial characteristics of inulin-responders in both *hum-ob* mice and human cohort.

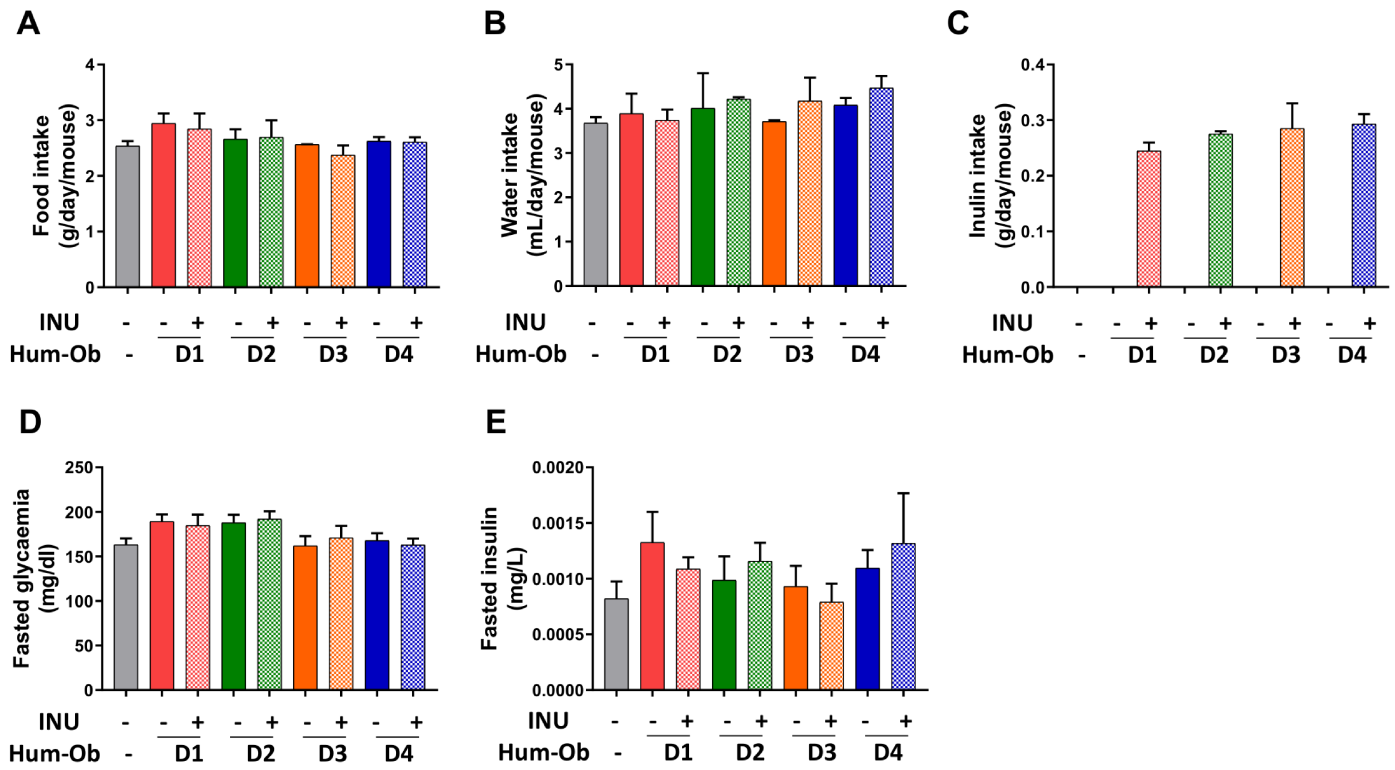
In *hum-ob* mice model, inulin decreased *Victivallis*, *Butyricimonas*, *Bilophila*, *Barnesiella* and *Hungatella*, five genera correlated with detrimental metabolic features, in one group of inulin-responder mice.

In the second inulin-responder group in *hum-ob* mice, inulin supplementation increased the abundance of *Blautia*, *Akkermansia*, *Clostridium XIVa* and *Raoultella*, four genera negatively correlated with hepatic lipid accumulation. *Akkermansia*, *Clostridium XIVa* and *Raoultella* also negatively correlated with the expansion of SAT mass. The increase of *Blautia* and *Akkermansia* are also associated with the reduced intramuscular lipids accumulation.

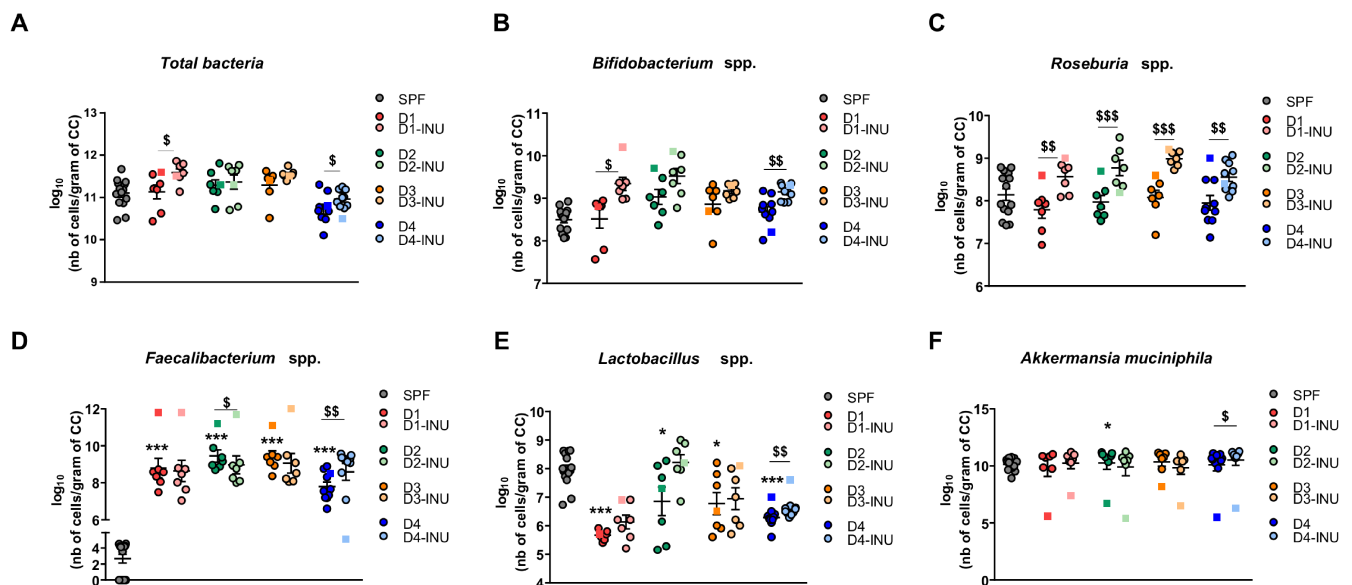
Finally, in the human cohort of obese individuals, the responder group in terms of BMI improvement was characterized by a higher abundance of *Akkermansia muciniphila* and *Butyricoccus* at baseline.

REFERENCES

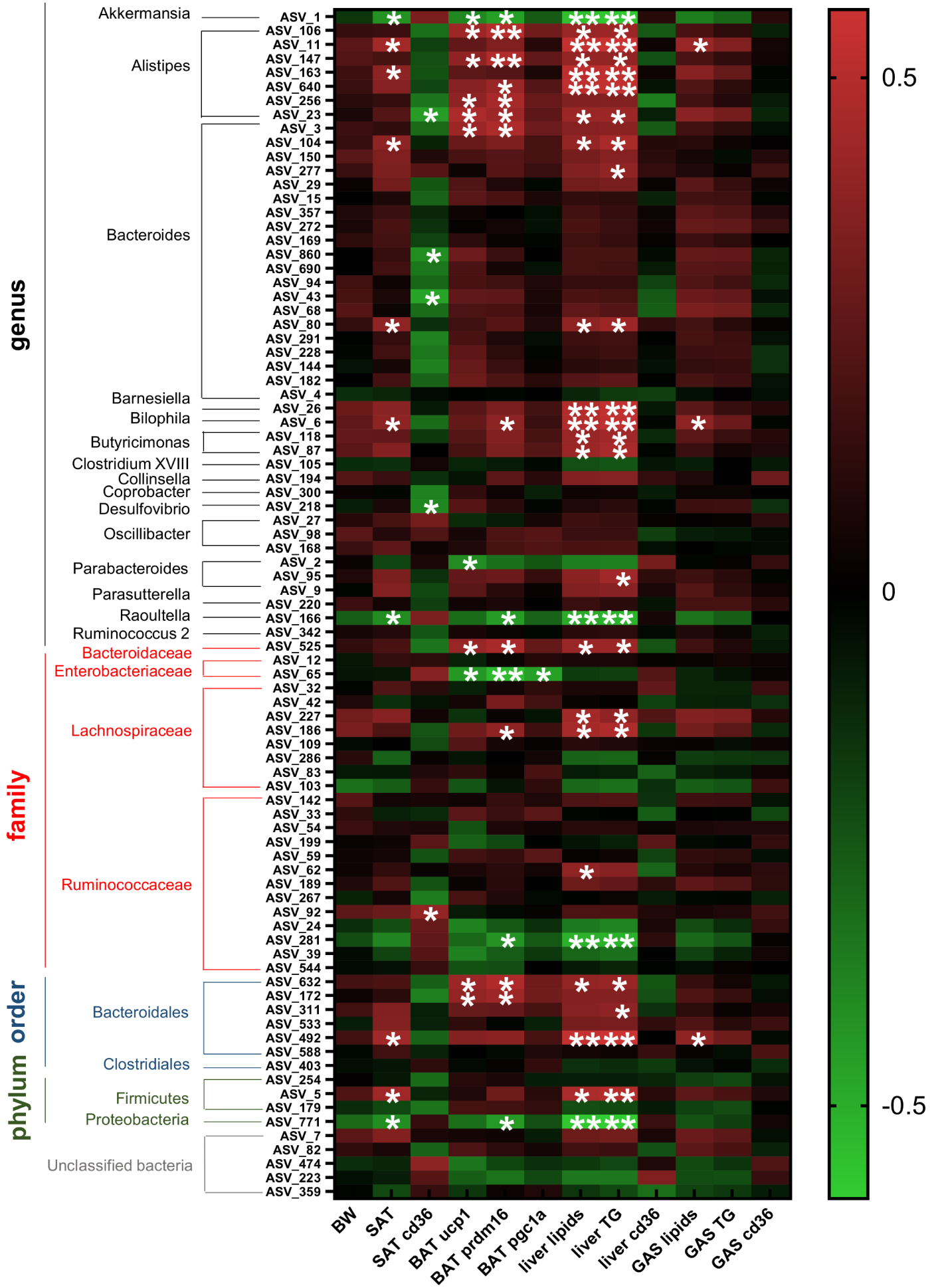
1. Le Roy T, Debedat J, Marquet F, et al. Comparative Evaluation of Microbiota Engraftment Following Fecal Microbiota Transfer in Mice Models: Age, Kinetic and Microbial Status Matter. *Front Microbiol* 2018;9:3289. doi: 10.3389/fmicb.2018.03289 [published Online First: 2019/01/30]
2. Reikvam DH, Erofeev A, Sandvik A, et al. Depletion of murine intestinal microbiota: effects on gut mucosa and epithelial gene expression. *PLoS One* 2011;6(3):e17996. doi: 10.1371/journal.pone.0017996 [published Online First: 2011/03/30]
3. Folch J, Lees M, Sloane Stanley GH. A simple method for the isolation and purification of total lipides from animal tissues. *J Biol Chem* 1957;226(1):497-509. [published Online First: 1957/05/01]
4. Eren AM, Vineis JH, Morrison HG, et al. A filtering method to generate high quality short reads using illumina paired-end technology. *PLoS One* 2013;8(6):e66643. doi: 10.1371/journal.pone.0066643 [published Online First: 2013/06/27]
5. Schloss PD, Westcott SL, Ryabin T, et al. Introducing mothur: open-source, platform-independent, community-supported software for describing and comparing microbial communities. *Appl Environ Microbiol* 2009;75(23):7537-41. doi: 10.1128/AEM.01541-09 [published Online First: 2009/10/06]
6. Edgar RC. UPARSE: highly accurate OTU sequences from microbial amplicon reads. *Nat Methods* 2013;10(10):996-8. doi: 10.1038/nmeth.2604 [published Online First: 2013/08/21]
7. Wang Q, Garrity GM, Tiedje JM, et al. Naive Bayesian classifier for rapid assignment of rRNA sequences into the new bacterial taxonomy. *Appl Environ Microbiol* 2007;73(16):5261-7. doi: 10.1128/AEM.00062-07 [published Online First: 2007/06/26]
8. Caporaso JG, Kuczynski J, Stombaugh J, et al. QIIME allows analysis of high-throughput community sequencing data. *Nat Methods* 2010;7(5):335-6. doi: 10.1038/nmeth.f.303 [published Online First: 2010/04/13]
9. Benjamini Y HY. Controlling the False Discovery Rate : A Practical and Powerful Approach to Multiple Testing. . *Journal of the Royal Statistical Society* 1995;57:289-300.



Supplemental Figure 1



Supplemental Figure 2



Supplemental Figure 3

